Electronic Supplementary Material (ESI) for Environmental Science: Water Research & Technology.
This journal is © The Royal Society of Chemistry 2022

Engineered Osmosis - sustainable technology for water recovery, product concentration and energy generation

Noel Jacob Kaleekkal[a]*, Jenny Nambikkattu[a], Ajmal Rasheeda Satheesh[a], Ralph Rolly Gonzales[b,c], Ho Kyong Shon[b], Saravanamuthu Vigneswaran[b*],

[a] Membrane Separation Group, Department of Chemical Engineering, National Institute of Technology Calicut, Kozhikode, Kerala -673601, India
[b] Centre for Technology in Water and Wastewater, School of Civil and Environmental Engineering, University of Technology Sydney, Sydney, NSW 2007, Australia
[c] Research Center for Membrane and Film Technology, Kobe University, Kobe, Hyogo 657-8501 Japan

Corresponding authors e-mail: noeljacob89@gmail.com, noel@nitc.ac.in, Saravanamuth.Vigneswaran@uts.edu.au

List of Tables

List of figures

Tables

Table S1. Novel draw solutes and their regeneration methods

Sl. No.	Draw solute	Example	Regeneration method	References
1	Inorganic salts	NH_4HCO_3	Thermal decomposition	[1]
2	Magnetic nanoparticles (MNPs)	Branched poly (deep eutectic solvent)@Fe_3O_4	Magnetic field	[2]
3	Polymer hydrogel	poly(sodium acrylate, PSA) poly (N-isopropylacrylamide) (PNIPAm)	Deswelling	[3]
4	Thermoresponsive magnetic nanoparticle	Magnetite functionalized with poly(N-isopropyla- crylamide) and triethylene glycol (PNIPAM/TRI-MNP)	Magnetic attraction after mild heating	[4]
5	Fertilizers	Ammonium chloride, Potassium chloride, Ammonium sulphate, and Calcium nitrate	None	[5]
6	Polyelectrolyte	Sodium salts of poly- acrylic acid PAA-Na	Ultrafiltration	[6]
7	Hydro acid complexes	Cupric and ferric complexes with hydroxyl acids of citric acid (CA), malic acid (MA), and tartaric acid (TA) as	Nanofiltration	[7]
8	Carbon quantum dots	Na^+ -functionalized carbon quantum dots	Membrane distillation	[8]

Figures

Figure. S1 Commercial FO membrane and system suppliers in the world

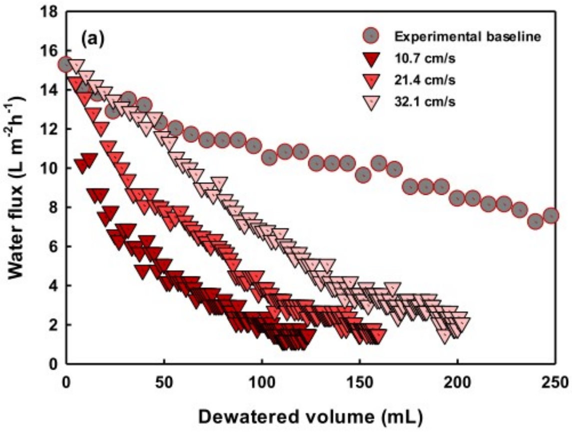

Fig. S2. Effect of pre-treatment strategies- (a) hydraulic fouling control (increasing cross-flow velocity) (b) sedimentation and centrifugation on the flux decline during grapefruit juice dehydration. 2 M NaCl was employed as the draw solution. The experimental baseline represents the flux decline due to the dilution of the draw solution.

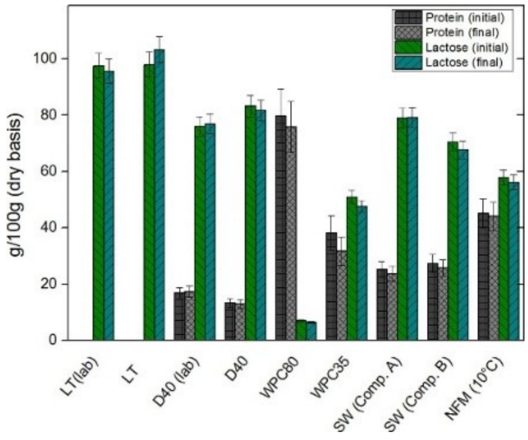

Fig. S3. The concentration of protein and lactose on a dry basis before and after FO experiments. (LT: lactose, D40: demineralized whey with 40% mineral removal, WPC35 and WPC80: whey protein concentrate with a protein content of 35% and 80%; SW: sweet whey; NFM: non-fat milk).

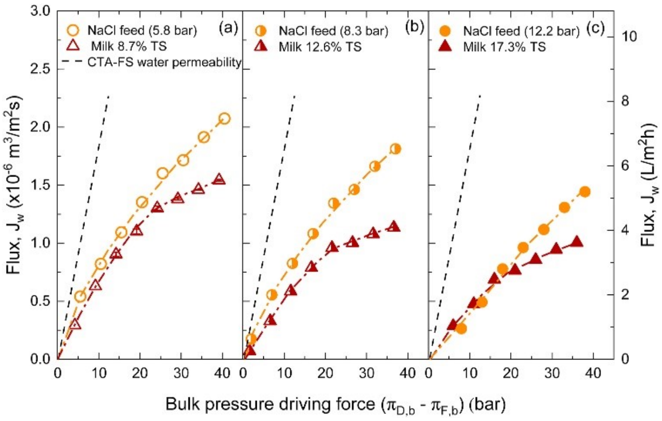

Fig. S4. Flux as a function of bulk osmotic pressure driving force in step-pressure forward osmosis (FO) mode for (a) fresh milk with 8.7% total solids (b) milk with 12.6% total solids and (c) milk with 17.6% total solids; milk cross-flow velocity of 0.2 m/s.

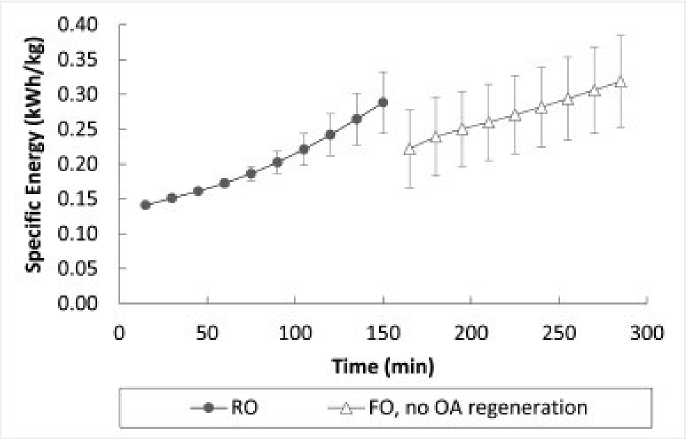

Fig. S5. Specific cumulative energy consumption (kWh/kg water removed) over time for the combination of RO and FO of Greek style acid whey (GAW)

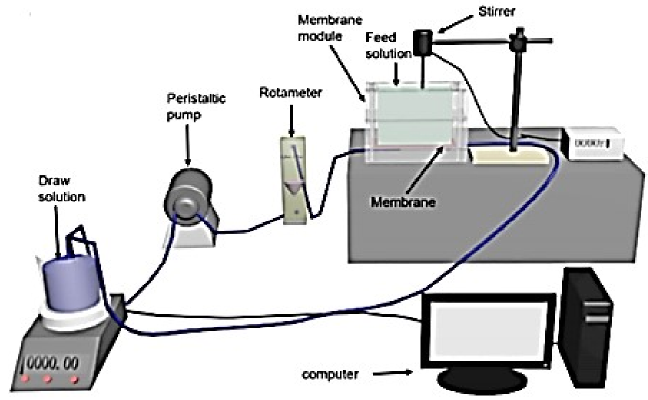

Figure S6. Schematic diagram of a hybrid dead-end/cross-flow forward osmosis system

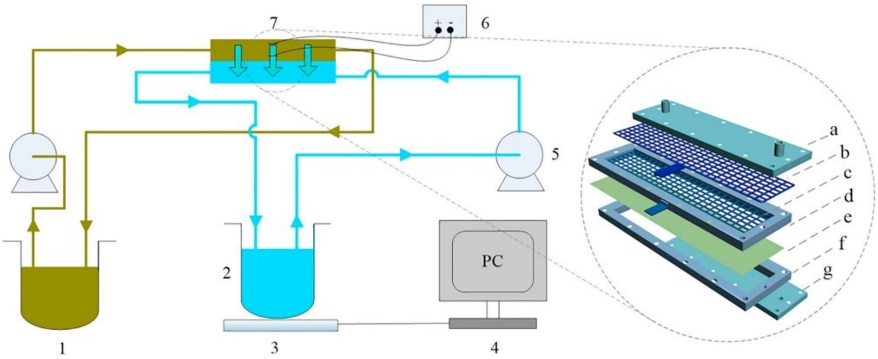

Fig. S7. The flow diagram of the bench-scale FO-EO process and internal schematic of the FO-EO reactor (1 Feed solution tank; 2 Draw solution tank; 3 Digital balance; 4 Computer; 5 Peristaltic pump; 6 DC power supply; 7 FO-EO reactor. a Top plate; b Anode; c Cathode; d and f Silicone spacers; e FO membrane; g Bottom plate).

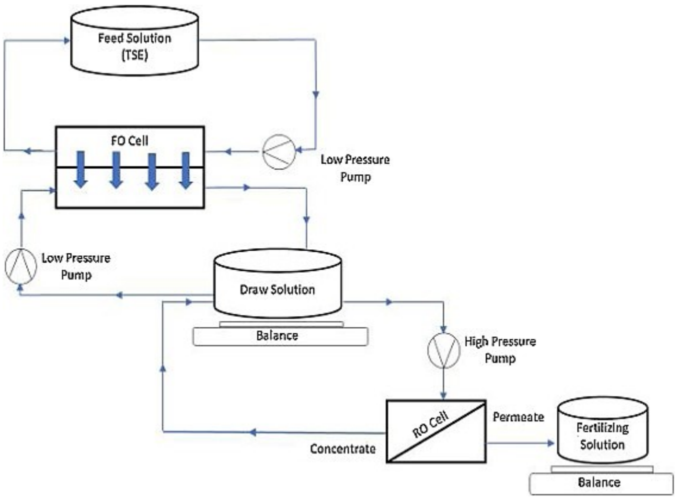

Fig. S8. Integrated FO-RO system for the production of fertilizing solution.

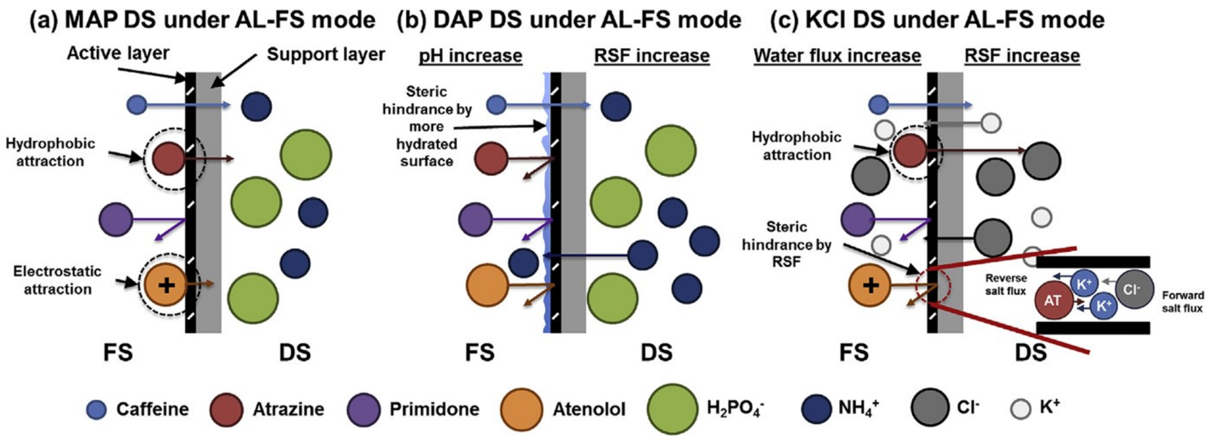

Fig. S9. Schematic descriptions of OMPs transport mechanisms in FO.

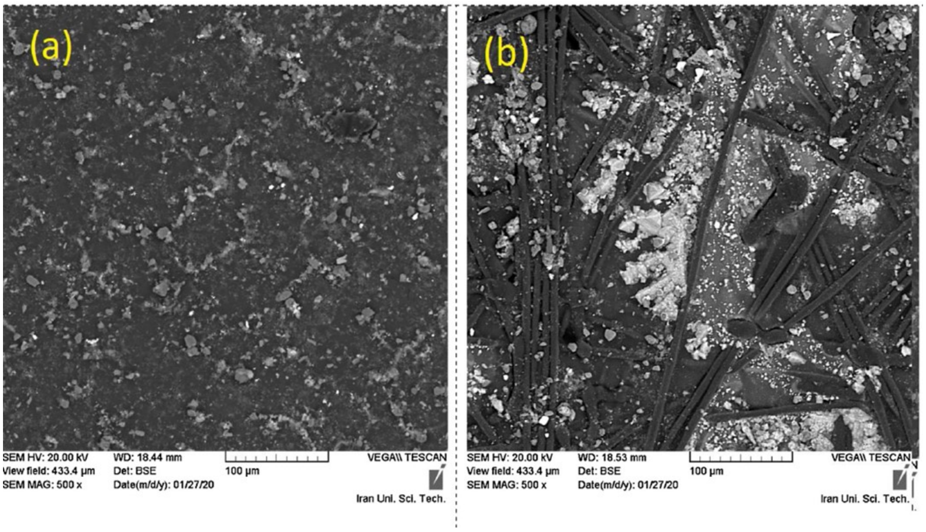

Figure S10. SEM images top and bottom surface of aquaporin membrane after FO filtration with oily wastewater.

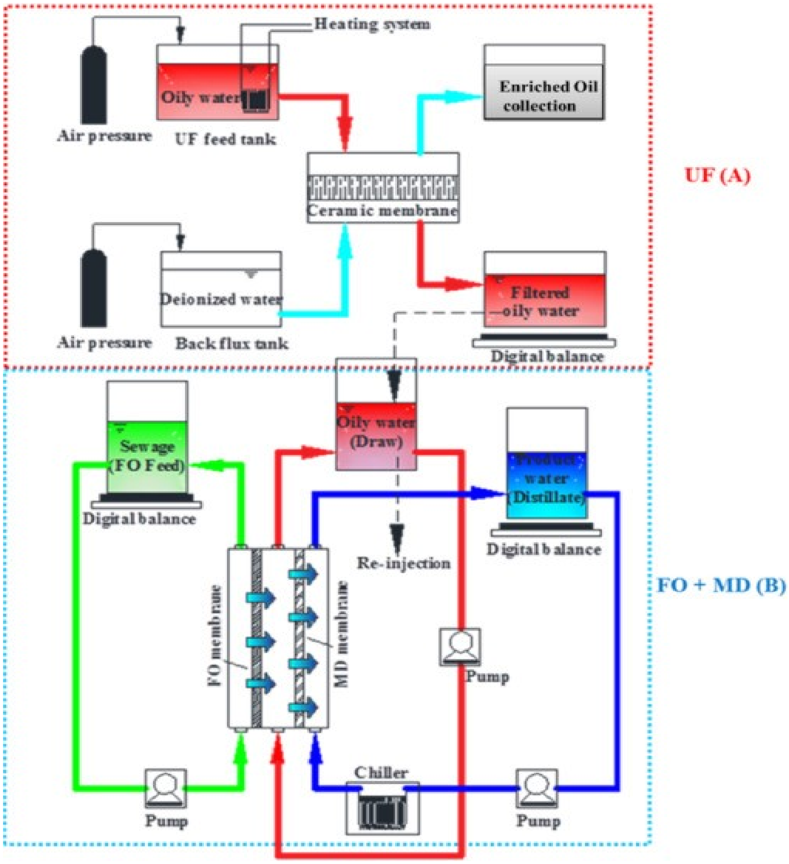

Fig. S11. Integrated FO-MD-UF system.

1. Theory

1.1.1 Membrane orientation in forward Osmosis- FO and PRO mode

If the active layer (selective layer) of the membrane is in contact with the feed solution and the porous sublayer is in contact with the draw solution, this configuration is termed FO mode. When the membrane orientation is reversed, it is termed as PRO mode.

The water flux through the membrane can be calculated by eq. 1

$$J_W = A\left[\left(\pi_{D,b} - \pi_{F,b}\right) - \Delta P\right] \qquad (1)$$

$$J_s = B\left(C_{Db} - C_{Fb}\right) \qquad (2)$$

where *A* is pure water permeability; *B* is solute permeability; σ=1, and no *ΔP* across the membrane.

A and B are both intrinsic to the membrane considered. A higher value of A corresponds to higher water flux and B must be as low as possible as it corresponds to reverse salt flux from draw solution to the feed solution, which is undesirable. The water flux increases with the increase in draw solution concentration due to a greater driving force [9].

However, it was observed that in most reports, the flux in the membrane orientation in which the active layer facing draw solution (ALDS) is higher than the active layer facing feed solution (ALFS) orientation; sometimes, an order of magnitude greater, which could be due to the lower internal concentration polarization (ICP) [10]. The membrane orientation has to be evaluated in greater detail as the ALDS mode often encounters higher reverse solute flux, indicating the loss of draw solute and contamination of the feed solution [11]. In some cases, it can be observed that flux decline was more pronounced and higher in the PRO mode since (i) higher flux lowers the driving force ($\Delta\pi$), and (ii) higher internal concentration polarization (in support) due to the foulants in the feed [12].

1.1.2. Concentration polarization

In ALFS mode (FO configuration), an accumulation of rejected salts at the active layer gives rise to concentrative external concentration polarization (CECP). As the water permeates through the support, it dilutes the draw solution leading to dilutive internal concentration polarization (DICP). In the ALDS mode (PRO configuration), rejected salts accumulate within the support layer as water permeates across the membrane, leading to concentrative internal concentration polarization (CICP). The water further carries away the draw solute at the interface of the active layer giving rise to dilutive external concentration polarization (DECP). This is illustrated in Fig. 2

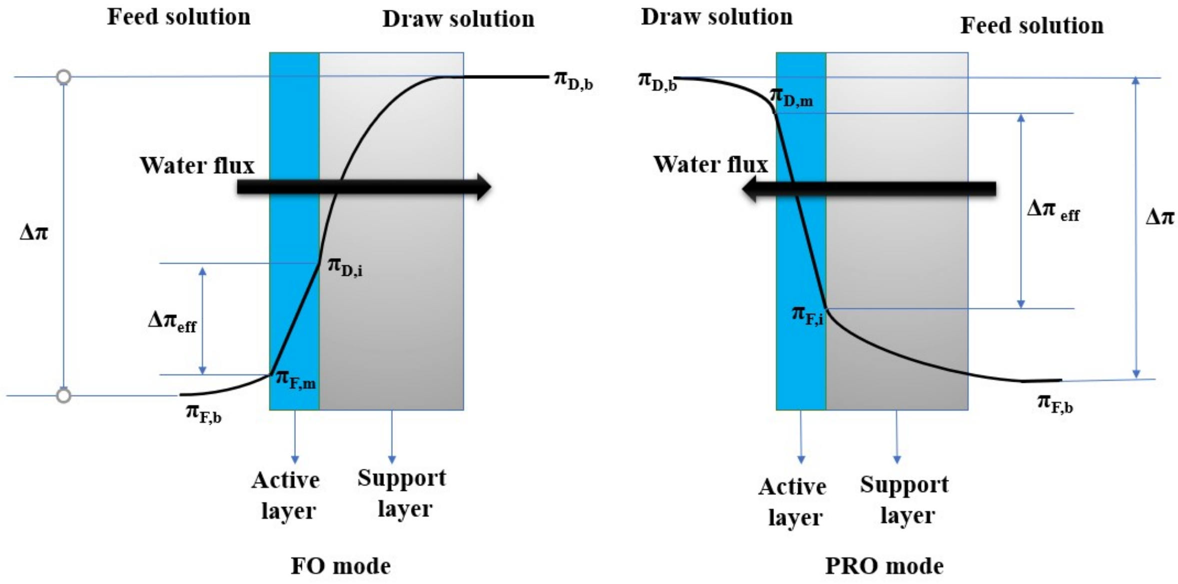

Fig. S12. Illustration of osmotic driving force profiles in PRO and FO modes. (a) The profile illustrates concentrative ECP and dilutive ICP for FO mode. (b) The profile illustrates dilutive ECP and concentrative ICP in PRO mode. Key: $\pi_{D,b}$ is the bulk draw osmotic pressure, $\pi_{D,m}$ is the membrane surface osmotic pressure on the draw solution side, $\pi_{F,b}$ is the bulk feed osmotic pressure, $\pi_{F,m}$ is the membrane surface osmotic pressure on the feed side, $\pi_{F,i}$ is the effective osmotic pressure of the feed in PRO mode, $\pi_{D,i}$ is the effective osmotic pressure of the draw solution in FO mode, and $\Delta\pi_{eff}$ is the effective osmotic driving force.

The observed water flux would be generally lower than the theoretical value (eq 1) due to the concentration polarization on the membrane surface or within the support. The osmotic pressures at the membrane interfaces have to be included in calculating the theoretical flux. This can be carried out following the method outlined by McCutcheon et al.[13], using the appropriate Sherwood correlation (eq. 3& 4).

$$Sh = 1.85\left(Re\, Sc\frac{d_h}{L}\right)^{0.33} \quad \text{(Laminar flow)} \qquad (3)$$

$$Sh = 0.04\, Re^{0.75} Sc^{0.33} \quad \text{(Turbulent flow)} \qquad (4)$$

where *Sh* is the Sherwood number, *Re* is the Reynolds number, and *Sc* is the Schmidt number. The terms d_h and L correspond to the hydraulic diameter and the length of the channel, respectively and are specific to the membrane module . The mass transfer coefficient k is evaluated from the Sherwood number (eq 5),

$$k = \frac{Sh\, D}{dh} \tag{5}$$

where D is the coefficient of solute diffusivity of the particular solute. The value obtained can be plugged to eq 6 to obtain the concentrative ECP modulus

$$\frac{\pi F,m}{\pi F,b} = \exp\left(\frac{Jw}{k}\right) \tag{6}$$

with $\pi_{F,m}$- Osmotic pressure of feed solution at the membrane surface and $\pi_{F,b}$- Osmotic pressure of feed solution in bulk. An assumption made here is that the ratio between the osmotic pressures is equal to the corresponding ratio between their concentrations in the solution, which is a safe assumption for dilute solutions. Further, the assumption that $\pi_{F,m} > \pi_{F,b}$ is valid due to the CECP occurring.

The effect of ICP could be determined from the algorithm formulated by Lee et al. [14] and Loeb et al. [15] given in eq. 7:

$$K = \left(\frac{1}{J_\omega}\right) \ln \frac{B + A\pi_{D,m} - J_\omega}{B + A\pi_{F,b}} \tag{7}$$

where K is the solute resistivity, given by the eq. 8:

$$K = \frac{S}{D} \tag{8 a}$$

where S is the structural parameter of the membrane, K is a measure of how long it takes for the salt to diffuse out of the support layer and is a measure of the ICP. The structural parameter is introduced to quantify the influence of membrane porosity and is expressed as:

$$s = \frac{t\tau}{\varepsilon_b} \tag{8b}$$

where t is the thickness of the support layer, τ is the tortuosity, and ε_b is the bulk porosity of the support layer.

The CICP modulus is calculated assuming no salt is transported across the membrane

$$\frac{\pi_{F,i}}{\pi_{F,b}} = \exp(J_w K) \tag{9}$$

where $\pi_{F,i}$ is the osmotic pressure of feed solution at the bottom of the AL as shown in Figure 2. Similarly, to calculate the DICP modulus the solute resistivity is calculated [15] (eq. 10):

$$K = \left(\frac{1}{J_\omega}\right) \ln \frac{B + A\pi_{D,b}}{B + A\pi_{F,m} + J_\omega} \tag{10}$$

Using the same assumptions as used for CICP that is, salt flux being negligible. Then the DICP modulus can be written as:

$$\frac{\pi_{D,i}}{\pi_{D,b}} = \exp(-J_w K) \tag{11}$$

where $\pi_{D,i}$ is the osmotic pressure of draw solution on the inside of the membrane. Using the appropriate CP moduli, then the equation for water flux can be re-written as:

$$J_w^{FO} = A\left\{\pi_{D,b} \exp(-J_w K) - \pi_{F,b} \exp\left[\frac{J_w}{k}\right]\right\} \tag{12}$$

$$J_w^{PRO} = A\left\{\pi_{D,b} \exp\left[-\frac{J_w}{k}\right] - \pi_{F,b} \exp(J_w K)\right\} \tag{13}$$

And the reverse salt flux can be written as :

$$\mathrm{J_s}^{\mathrm{FO}} = \mathrm{B}\left\{ \mathrm{CD,b}\,exp\left[\left(-J_w K\right)\right] - \mathrm{CF,b}\,exp\left[\frac{J_w}{k}\right] \right\} \tag{14}$$

$$\mathrm{J_s}^{\mathrm{PRO}} = \mathrm{B}\left\{ \mathrm{CD,b}\,exp\left[-\frac{J_w}{k}\right] - \mathrm{CF,b}\,exp\left(J_w K\right) \right\} \tag{15}$$

References

[1] L. Feng, L. Xie, G. Suo, X. Shao, and T. Dong, "Influence of Temperature on the Performance of Forward Osmosis Using Ammonium Bicarbonate as Draw Solute," *Trans. Tianjin Univ.*, vol. 24, no. 6, pp. 571–579, 2018, doi: 10.1007/s12209-018-0159-1.

[2] Y. Bide and S. Shokrollahzadeh, "Toward tailoring of a new draw solute for forward osmosis process: Branched poly (deep eutectic solvent)-decorated magnetic nanoparticles," *J. Mol. Liq.*, vol. 320, no. December, p. 114409, 2020, doi: 10.1016/j.molliq.2020.114409.

[3] J. Wang, S. Gao, J. Tian, F. Cui, and W. Shi, "Recent developments and future challenges of hydrogels as draw solutes in forward osmosis process," *Water (Switzerland)*, vol. 12, no. 3, pp. 1–20, 2020, doi: 10.3390/w12030692.

[4] M. M. Ling, T. Chung, and X. Lu, "Facile synthesis of thermosensitive magnetic nanoparticles as '"smart"' draw solutes in forward osmosis," vol. 47, no. september 2011, pp. 10788–10790, 2011, doi: 10.1039/c1cc13944d.

[5] S. Phuntsho, H. K. Shon, S. Hong, S. Lee, S. Vigneswaran, and J. Kandasamy, "Fertiliser drawn forward osmosis desalination: The concept, performance and

limitations for fertigation," *Rev. Environ. Sci. Biotechnol.*, vol. 11, no. 2, pp. 147–168, 2012, doi: 10.1007/s11157-011-9259-2.

[6] Q. Ge, J. Su, G. L. Amy, and T. Chung, "Exploration of polyelectrolytes as draw solutes in forward osmosis processes," *Water Res.*, vol. 46, no. 4, pp. 1318–1326, 2011, doi: 10.1016/j.watres.2011.12.043.

[7] T.-S. C. Qingchun Ge, "Hydroacid complexes: a new class of draw solutes to promote forward osmosis (FO) processes," *Chem. Commun.*, vol. 4, no. 76, pp. 8471–8473, 2013, doi: 10.1039/c3cc43951h.

[8] P. W. and X. L. Chun Xian Guo,‡ Dieling Zhao,‡ Qipeng Zhao, "Na + -functionalized carbon quantum dots : a new draw solute in forward osmosis for seawater desalination," *Chem. Commun*, vol. 50, no. may 2014, pp. 7318–7321, 2014, doi: 10.1039/c4cc01603c.

[9] R. R. Gonzales, L. Zhang, Y. Sasaki, W. Kushida, H. Matsuyama, and H. K. Shon, "Facile development of comprehensively fouling-resistant reduced polyketone-based thin film composite forward osmosis membrane for treatment of oily wastewater," *J. Memb. Sci.*, vol. 626, no. January, p. 119185, 2021, doi: 10.1016/j.memsci.2021.119185.

[10] X. Wu *et al.*, "Improved Performance and Mitigated Internal Concentration Polarization of Thin-Film Composite Forward Osmosis Membrane with Polysulfone/Polyaniline Substrate," *J. Mater. Chem. A Mater. energy Sustain.*, vol. 00, no. June, pp. 1–10, 2018, doi: 10.1039/C8TA01200H.

[11] S. Liu *et al.*, "Multi-functional tannic acid (TA)-Ferric complex coating for forward osmosis membrane with enhanced micropollutant removal and antifouling property," *J. Memb. Sci.*, vol. 626, no. February, p. 119171, 2021, doi: 10.1016/j.memsci.2021.119171.

[12] J. Chang *et al.*, "Efficient organic enrichment from sludge filtrate via a forward osmosis membrane process," *J. Environ. Chem. Eng.*, vol. 8, no. 4, p. 104042, 2020, doi: 10.1016/j.jece.2020.104042.

[13] J. R. McCutcheon, R. L. McGinnis, and M. Elimelech, "Desalination by ammonia-carbon dioxide forward osmosis: Influence of draw and feed solution concentrations on process performance," *J. Memb. Sci.*, 2006, doi: 10.1016/j.memsci.2005.10.048.

[14] K. L. Lee, R. W. Baker, and H. K. Lonsdale, "Membranes for power generation by pressure-retarded osmosis," *J. Memb. Sci.*, vol. 8, no. 2, pp. 141–171, 1981, doi: 10.1016/S0376-7388(00)82088-8.

[15] S. Loeb, L. Titelman, E. Korngold, and J. Freiman, "Effect of porous support fabric on osmosis through a Loeb-Sourirajan type asymmetric membrane," *J. Memb. Sci.*, vol. 129, no. 2, pp. 243–249, 1997, doi: 10.1016/S0376-7388(96)00354-7.